American Journal of Mechanical and Materials Engineering
2024, Vol. 8, No. 3, pp. 47-54
https://doi.org/10.11648/j.ajmme.20240803.12

Research Article

Modeling the Dynamics of Quasi-Zero Stiffness Vibration Isolator of Shape Memory Alloy Spring Using Matlab Software

Rabiu Ahmad Abubakar*

Department of Mechanical Engineering, Zhejiang University, Hangzhou, China

Abstract

This study investigates the dynamic behavior of a quasi-zero stiffness (QZS) vibration isolator integrated with shape memory alloy (SMA) springs to achieve enhanced vibration isolation performance. QZS isolators are designed to mitigate vibrations effectively in low-frequency environments by combining linear and nonlinear stiffness elements to achieve a near-zero effective stiffness around the equilibrium position. The inclusion of SMA springs introduces unique properties such as shape memory effect and pseudoelasticity, enabling tunable stiffness and damping characteristics.. A comprehensive mathematical model of the isolator is developed, incorporating the nonlinear force-displacement behavior of the SMA spring based on thermomechanical coupling and constitutive relations. The dynamics of the system are analyzed under harmonic and random excitation, and key parameters influencing isolation performance, such as temperature, pre-compression of the SMA spring, and system damping, are systematically explored. Numerical simulations reveal that the SMA-based QZS isolator exhibits superior vibration attenuation compared to traditional isolators, with the added benefit of adaptability to changing operational conditions. It is demonstrated that the resonant frequency of the proposed isolation system is near zero. Numerical simulations are carried out, and the influence of the excitation amplitude and frequency on vibration isolation are studied. It is shown that a quasi-zero dynamic stiffness is achieved; hence the feasibility of the proposed system for low-frequency excitation isolation is validated.

Keywords

Vibration Isolation, Shape Memory Alloys, Martensite Transformation, Pseudoelasticity

1. Introduction

With the advancement of modern industry, the requirement for vibration isolation of precise instruments and important apparatus has been more and more rigid and demanding [1]. The natural frequency of the vibration isolation is made lower than the vibration excitation frequency to enhance the vibration isolation performance. Hence the stiffness of the isolation system should be small. Meanwhile, the isolation system need also be capable of supporting the system weight to be isolated in a static state. This means the spring stiffness has to be strong enough to support the mass. This contradiction thus makes the design of frequency vibration very challenging. Particularly when the excitation frequency is low, The stiffness dynamic of the spring should be as low as possible to reduce its natural frequency in the ultra-low region. This fact

*Corresponding author: rbkiru@yahoo.com (Rabiu Ahmad Abubakar)

Received: 11 November 2024; **Accepted:** 25 November 2024; **Published:** 19 December 2024

makes the use of linear springs completely unfeasible for ultra-low frequency vibration isolation. Since the ultra-low stiffness of the spring demanded by low natural frequency will cause unacceptably large static deflection [2]. To fit this need, the spring used in the vibration isolation must have a high-static stiffness while the low dynamic stiffness (HSLDS) has low stiffness to support a large load [3]. HSLDS is a nonlinear spring. Quasi-stiffness (QZS) means to have zero or near-zero dynamic stiffness. Many investigations on the concept of composite and nonlinear viscoelastic isolators have been published. Some researchers have designed a series of innovative units with quasi-zero stiffness.

An isolation system is introduced by Thanh Danh Le [4]. It has two symmetric negative stiffness structures in parallel with a positive stiffness structure. The system is applied in a vehicle seat. N. Zhou and K. Liu [5] designed a system which is connected to a mechanical spring in parallel to a magnetic spring. It consists of electromagnets and a permanent magnet. This isolator has a high-static-low-dynamic characteristic. Garoi *et al*. [6] used Roberts linkage [7] and built an ultra-low-frequency passive vibration isolation system. It is used as a pre-isolation stage for the Australian International Gravitational Observatory. These designs can achieve quasi-zero or quasi-negative stiffness by combining several springs in a specific way, but the related structure is quite complex.

The concept of the QZS isolator may be realised by combining a positive and negative stiffness mechanism together, such as common elastic elements. Alabuzhev [8] gives a detailed review of relevant design features, theory, and design methods. Anyone interested can refer to the book.

Many researchers are dedicated to the inclined spring to offer the negative stiffness in order to counteract the positive stiffness. Carrella [9] studied force-displacement characteristics and forced transmissibility of a system with two oblique springs and gave an optimisation evaluation between geometry parameters and the dynamic stiffness of such a system. Some researchers are making some improvements to this kind of QZS structure. Krishna [10] adds a semi-active damper to achieve better damping force than a skyhook configuration. Sun [11] adds a time-delayed active control to the system to reinforce the structural stability. Zhou [12] also design a QSZ. Isolator using for horizontal spring, just doing a little change in the contact type. He considers a roller-cam-spring structure which is also an alternative to the existing device with better performance than the linear counterpart. Latter, Zhou [13] employed the same mechanism to attenuate the transmissibility of torsional vibration and achieved the QZS property.

Others are pursuing other structures to offset the system's negative stiffness. A design by Carrella has a high-static-low-dynamic isolator comprised of two vertical mechanical springs between which an isolated mass is mounted while a magnet attaches to the outer edge of each mechanical spring. A negative magnetic spring developed by Zheng [14] comprises a pair of a permanent magnetic spring to counteract a mechanical spring with positive stiffness. Sun and Jing [15] add symmetrically scissor-like structures (SLS) acting as a mechanism with negative stiffness to work in parallel with a vertical ordinary spring-mass damper system placed in a vertical position to get a positive stiffness; thus, the whole device possesses the characteristic of a quasi-zero-stiffness. Another magnetic spring system designed by Zhou [13] consists of two permanent magnet and electromagnets to get a passive negative stiffness, while the mechanical spring is made up of a structural beam leaving out the hardening effect. The device designed by him also enlightened the semi-active vibration isolation.

Although the system demonstrated desirable QSZ characteristics and better performance than the traditional linear isolator, there are still some disadvantages to the current QZS system. First, some delicate structures are somehow complex and sophisticated. On the other hand, parameters of the QZS systems should be deliberately selected to drive the system away from its static instability caused by the negative stiffness mechanism.

Due to their internal nonlinearity and variable material property, nonlinear natural rubber and some smart materials are promising alternatives for constructing quasi-zero stiffness springs, and they are very good candidates for ultra-low frequency vibration isolation. Among well-investigated smart materials, shape memory alloy might be the best choice for vibration isolation and damping due to its shape memory effects and pseudoelasticity [16]. Yiu [17] applied shape memory alloy isolator in space devices and has proved the feasibility of reducing the on-orbit disturbance for the moment wheel assembly. S. Saadat [18] used shape memory alloy material to develop a new fastener mechanism that can greatly mitigate the damage of hurricanes caused on coastal structures. K. Williams [19] designed a new type of adaptively tuned vibration absorber that incorporated SMA as its spring element, and test results show the potential of SMA as the tuning element for vibration control strategies. C. Lagoudas [20] has conducted a series of researches to study pseudoelastic SMA spring elements for vibration isolation. An isolation device with an SMA tube as its spring element is constructed, and a modified Preisach model and a physically-based simplified SMA model are presented. Simulation and experiment results have shown its probability as an isolation element. Araki [21] integrated a super-elastic Cu-Al-Mn shape memory alloy bar into the tailored material design of a QZS isolator which converts the horizontal axial force of the SMA bar into the vertical recovery force.

Attracted by its unique pseudoelasticity and internal damping characteristics and the excellent recovery strain upon unloading displayed hysteresis and a near-flat stress plateau, a QZS isolator with high-static-low-dynamic property applying SMA spring as its loads-borne element can be easily obtained without any intricate mechanical design. Since vibration isolation is an inherently dynamic process, the modeling and analysis of the isolator certainly should be dynamic. In the

current paper, a differential model is proposed for the SMA spring by modeling the torsional motion of an SMA rod based on the Landau-Ginzburg free energy function. The dynamics of the SMA spring is computed as an ordinary differential equation, and the pseudoelastic behaviour and hysteresis loops are successfully captured. It is shown that the pseudo-elastic behaviour can dramatically change in the SMA spring stiffness and have a similar effect on vibration isolation of spring with a quasi-zero stiffness. Numerical simulations of the vibration isolation performance are presented.

2. Constitution Relationship of Torsional SMA Bar

In order to construct the model of the SMAs caused by phase transitions, the Landau-Ginzburg free energy function is employed here. The Lagrangian function, which comprises the sum of kinetic and potential energy contribution, is introduced to describe the mechanical field dynamics of SMAs [22].

$$L = \int_0^L (\frac{\rho}{2}(\dot{u})^2 - F)\, dx, \tag{1}$$

Where ρ is the material density, u stands for displacement, F stands for potential energy in form of force, while $\frac{\rho}{2}(\dot{u})^2$ is the kinetics energy density. Landau-Ginzburg is applied, which is a no-convex function of chosen order parameters and temperature θ. This function is split into two functions. The local energy density $F_1(\theta,\varepsilon))$ and non-local counterpart $F_g(\nabla\varepsilon)$. For this system, the strain is defined as $\varepsilon(x,t) = \frac{\partial u}{\partial x}$ and is chosen as local free energy density and is constructed based on Landau free energy density $F_1(\theta,\varepsilon)$ [23]:

$$F(\theta,\varepsilon) = \frac{K_1(\theta-\theta_c)}{2}\varepsilon^2 - \frac{K_2}{4}\varepsilon^4 + \frac{K_3}{6}\varepsilon^6, \tag{2}$$

Where θ is current temperature, k_1, k_2 and k_3 are the constants and θ_c is the critical transforming temperature. In this case, the non-local free density is constructed as $\frac{\partial\varepsilon}{\partial x}$ [24].

$$F_g(\nabla\varepsilon) = \frac{1}{2}k_g(\frac{\partial\varepsilon}{\partial x})^2 \tag{3}$$

Where k_g stand for material constant. Eqt. 3 is responsible for the inhomogeneous strain field. It is responsible for energy distribution from domain walls of different phases. For dissipation effects that go with phase transformation, a Rayleigh dissipation function is used as [24]:

$$F_R = \frac{1}{2}v(\frac{\partial u}{\partial t})^2 \tag{4}$$

Where v is the constant of the material, Eqt. 4 is responsible for internal friction between interfaces of different phases. It turns into the viscous effects of the phase transformation at macro-scale [24, 25].

Upon substituting the potential term into the Lagrangian function above, by applying Hamilton's principle [24], The mechanical field equation is obtained as:

$$\rho\ddot{u} = \frac{\partial}{\partial x}(k_1(\theta-\theta_c)\varepsilon + k_2\varepsilon^3 + k_3\varepsilon^5) + v\frac{\partial\partial^2 u}{\partial_t\partial x} - k_g\frac{\partial^4 u}{\partial x^4} \tag{5}$$

It is recast as:

$$\rho\ddot{u} = \frac{\partial\sigma}{\partial x} + v\frac{\partial\partial^2 u}{\partial_t\partial x} - k_g\frac{\partial^4 u}{\partial x^4},$$

$$\sigma = (k_1(\theta-\theta_c)\varepsilon + k_2\varepsilon^3 + k_3\varepsilon^5), \tag{6}$$

Eqt. 6 is the mechanical field for SMA rod [26].

In this paper, torsional stress is considered; therefore, the order parameter is substituted by the angular displacement u_x leading to the following equation:

$$\tau = (k_1(\theta-\theta_1)\gamma + k_2\gamma^3 + k_3\gamma^5) \tag{7}$$

Where τ is shear stress, k_1, k_2, *and* k_3 are material constants, γ is the torsional strain.

3. Modeling of Quasi-Zero-Stiffness SMA Spring

SMA spring modeling is derived in ref. [27]. With shape memory alloy spring as the elastic element of the isolation system, we are going to prove it can have a near-zero resonant frequency and be the perfect solution to the low-frequency vibration isolation.

For a simple one-layer vibration isolation system, as illustrated in Figure 1. It is a simple Mass-Spring-Damper (M-S-D) system, with the input of *Asin(wt)* acting the system as excitation. The effectiveness of the SMA spring as the vibration isolation component is examined later. The governing equation is:

$$m\ddot{x} + C\dot{x} + f = Asin(\omega t),$$

$$f = Asin(\omega t) - m\ddot{x} - C\dot{x}, \tag{8}$$

Where f is the SMA spring restoring force, and it is sinusoidal.

Numerical simulation is done in two parts. The first part gives a changing external excitation frequency and examines its dynamic response to different frequency inputs. Here we set m = 1 kg, c = 61N/(m/s), input frequency ω = 0-50 HZ. Figure 2 shows the result of the dynamic response corresponding to different frequencies. The simulation results show that a near-zero resonant frequency is obtained.

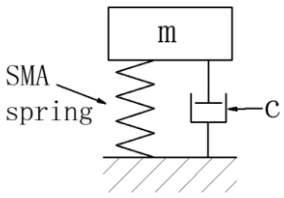

Figure 1. *Vibration system with SMA spring as isolation element.*

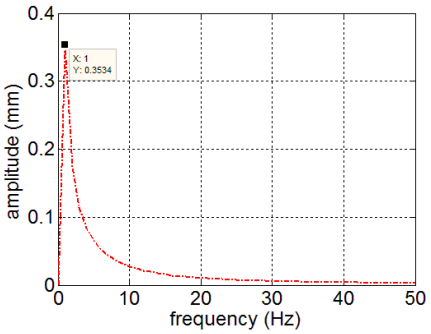

Figure 2. *Vibration system with SMA spring as isolation element.*

4. Estimation of Dynamic Stiffness

As to establish the feasibility of the SMA spring dynamic differential model, the concept of equivalent stiffness of SMA spring is introduced here 26, and is gotten as difference squared:

$$\int_{x_b}^{x_t}(F_s x - F_a x)^2 dx \tag{9}$$

where *Fs(x)* is SMA spring restoring force computed using Eq. 8, and F_a (x) = $k_e(x)$ is the linear force approximation and is calculated using the equivalent stiffness. The *xb* and *xt* are the minimal and maximum values for x. The estimated *ke* also depends on the choice of *xb* and *xt*.

In order to ensure the vibration reduction effect to utilize SMA's pseudoelasticity, the ambient temperature of the SMA spring is to be set above the Af, so the dependence of equivalent stiffness on the temperature is neglected. The equivalent stiffness *ke* is estimated in such a way that an ideal approximation to the nonlinear restoring force is *Fa(x) = ke(x)* in view of the least square error. Therefore, the approximation error function should be orthogonal to x, which gives the following relation:

$$F_s x - k_e x, x \geq 0 \tag{10}$$

Where < , > is the inner product of two functions on the specific domain. Given that the SMA spring displacement is not zero, which derives the following estimation of equivalent stiffness as stated:

$$k_e = \frac{<F_s x, x>}{\|x\|} \tag{11}$$

Equation 11 is a theoretical way to give a rough approximation of equivalent stiffness. As is known from the square error strategy, a sign of dependence of equivalent stiffness on a vibration amplitude is shown from the limit of integration. Several simulation estimations are given under different excitation magnitudes, which causes different vibration amplitudes. From the recovering force vs displacement diagram, a better approximation of equivalent stiffness is given by estimating the slope of the curve.

5. Simulation

Matlab software is used for the simulation. In the first, second and third simulations, the amplitude *A* =10, *A* =20, *A* =25 are used respectively, with applied force *f* = *2*, *f* = *10*, *f* = *20*, and *f* = 30, as to examine the dynamic response under the different magnitudes of excitation force, and the impact of input frequency on SMA spring stiffness as is shown in Figures 3-5, with the increasing level of excitation force, an overall increase of equivalent stiffness *ke* is checked, which means a positive correlation between input amplitude and equivalent stiffness *ke*.

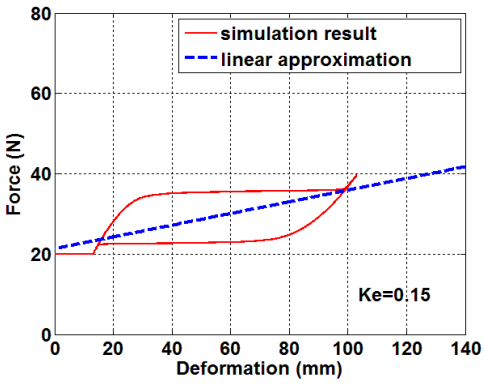

(a)

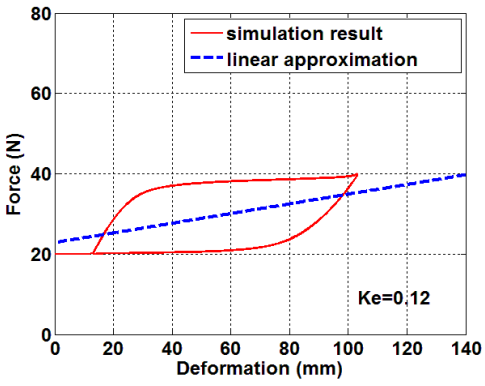

(b)

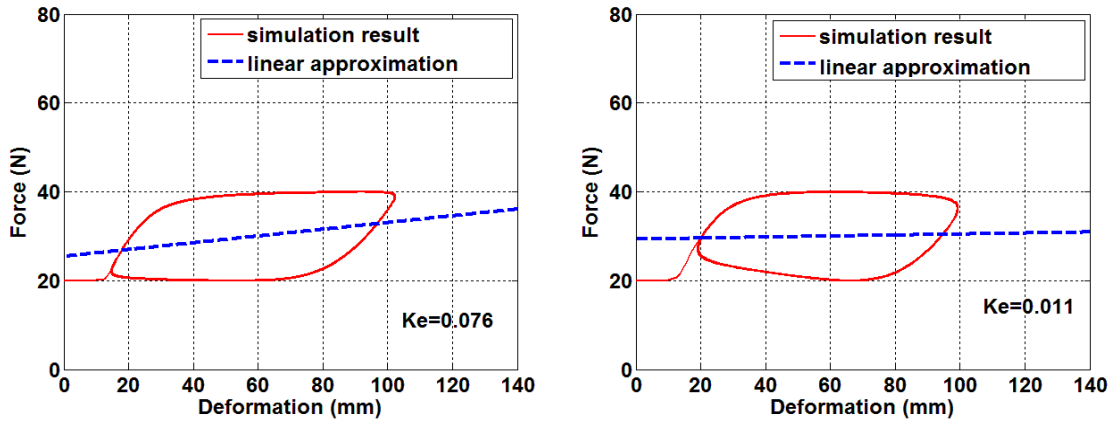

(c) (d)

Figure 3. *Equivalent stiffness under different excitation frequencies (a) f=2 (b) f=10 (c) f=20 (d) f=30 given the same excitation amplitude A=10.*

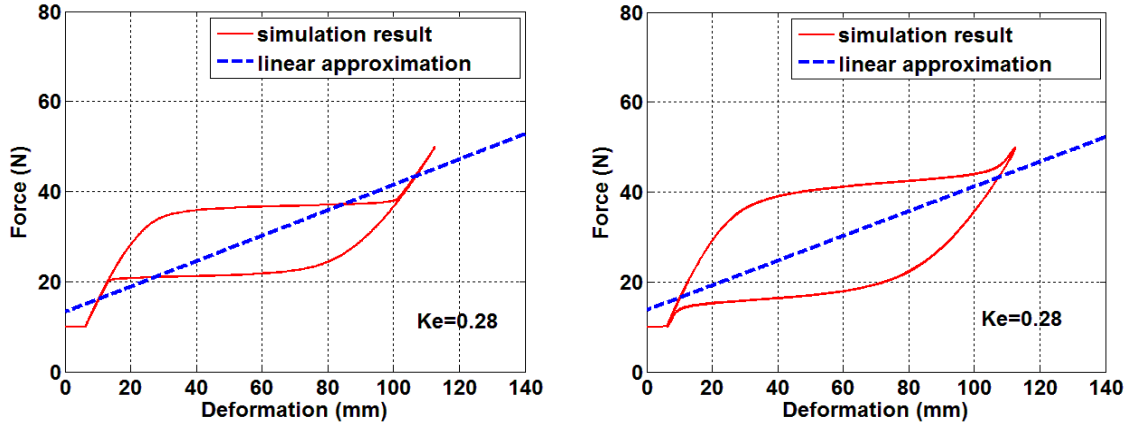

(a) (b)

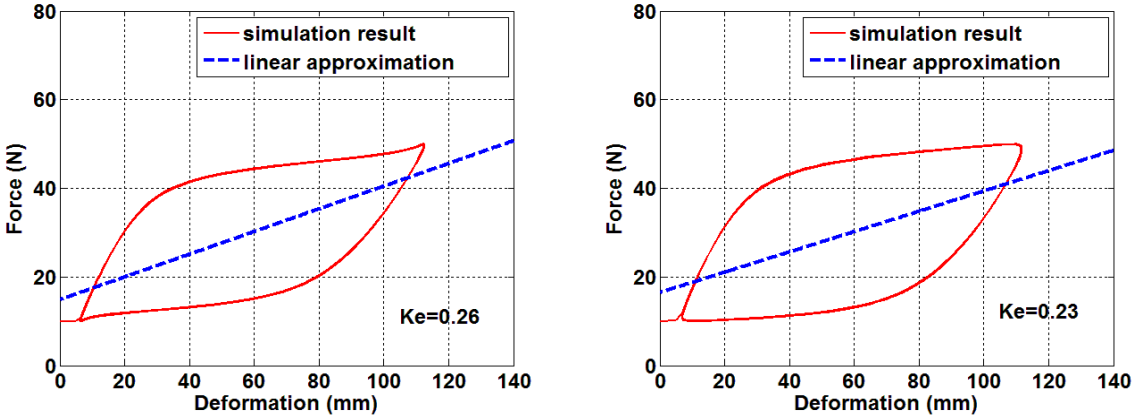

(c) (d)

Figure 4. *Equivalent stiffness under different excitation frequency (a) f=2 (b) f=10 (c) f=20 (d) f=30 given the same excitation amplitude A=20.*

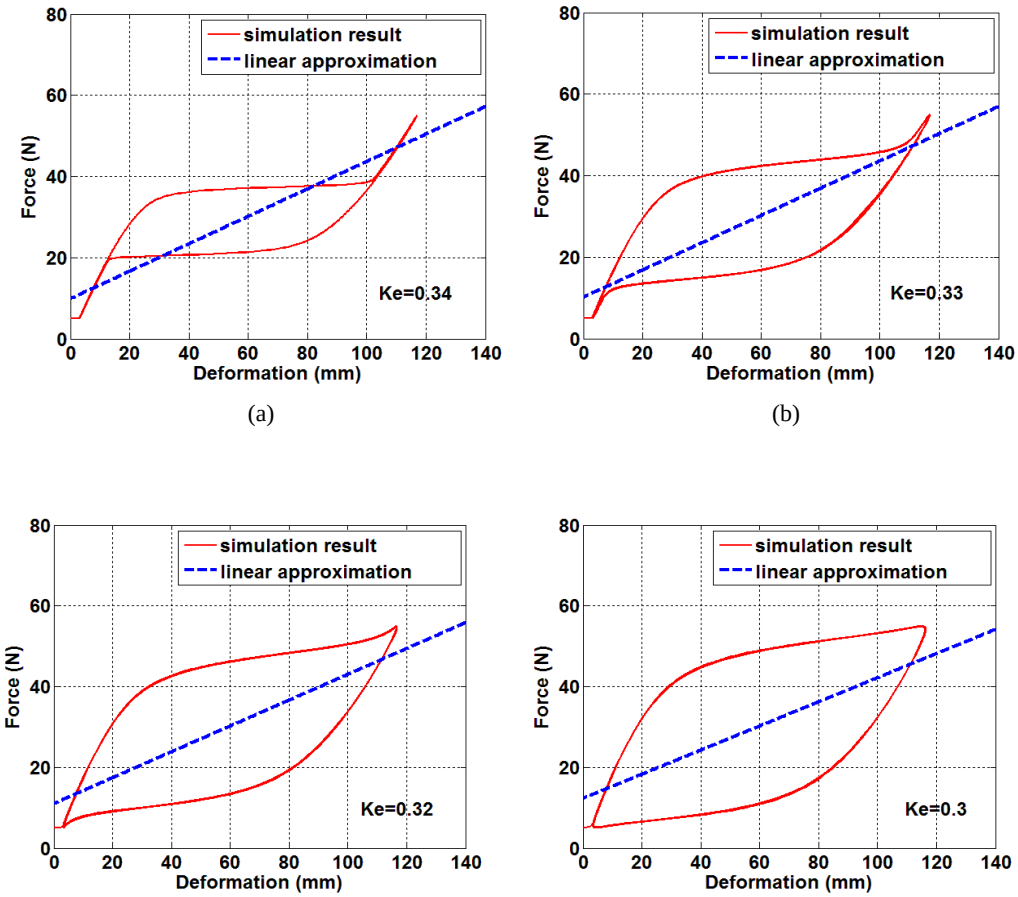

Figure 5. *Equivalent stiffness under different excitation frequency (a) f=2 (b) f=10 (c) f=20 (d) f=30 given the same excitation amplitude A=25.*

6. Discussion of Simulation Results

In the conducted simulations, the system's dynamic response was investigated under varying magnitudes of excitation force while maintaining different amplitude values. Here, the applied forces f =2, 10, 20, and 30 were considered for amplitudes A = 10, 20, and 25 to explore the behavior of the system. The findings are summarized and interpreted as follows:

Simulation with Amplitude A=10A = 10:

At this lower amplitude, the system displayed a relatively modest response, indicating that the smaller initial energy input resulted in limited excitation of the system's natural frequencies. As the applied force increased from f =2, f = 2 to f = 30, a progressive escalation in dynamic response was observed. Notably, nonlinear behaviors, if present, were less pronounced due to the smaller amplitude.

Simulation with Amplitude A=20A = 20:

For A = 20, A = 20, the increased amplitude introduced higher energy levels into the system, which amplified its sensitivity to the applied forces. At lower forces (f =2 and 10), the system maintained a quasi-linear response, with moderate oscillation magnitudes. However, as f = 20 and 30, the system exhibited significant dynamic effects, possibly indicating the onset of nonlinear phenomena such as resonance, depending on the frequency of the excitation force relative to the system's natural frequency.

Simulation with Amplitude A=25A = 25:

With A = 25, A = 25, the system was subjected to the highest amplitude, resulting in a strongly energized state. For f =2, f = 10, the responses were pronounced but remained within expected dynamic limits. As the force reached f = 20, f = 20 and f =30, the system's response demonstrated substantial oscillations, potentially approaching instability or chaotic behavior if the forcing frequency aligned with critical modes. This high amplitude setting likely highlighted any intrinsic nonlinearities in the system's dynamics, as observed in abrupt changes or bifurcations in the response pattern.

Observations:

Force-Amplitude Interaction: Across all amplitudes, the response intensified with increasing excitation force. This trend underscores the proportional relationship between applied force and system energy under linear conditions but also hints at nonlinear escalation in higher ranges.

Threshold Effects: For higher amplitudes and forces, there

may be thresholds beyond which the system shifts from stable oscillations to complex, potentially chaotic dynamics. Identifying these thresholds is critical for understanding system stability.

System Sensitivity: The dynamic response was significantly influenced by both amplitude and applied force, demonstrating the necessity of analyzing the system under combined variations for comprehensive characterization.

Another noticeable point is that the rate-dependent phenomenon can be seen within each level of input magnitude. The effect of input frequency on the hysteresis loop is shown and further affects the equivalent stiffness.

From the above simulation results, each one shows an equivalent stiffness of less than one. From the resonant frequency equation $\omega_n = \sqrt{\frac{k_c}{m}}$, a near-zero resonant frequency is obtained, which corresponds to the first part of the simulation. Thus the validity of our SMA spring model is proved. The trade-off between the capability of supporting objectives and the need to narrow down the vibration isolation natural frequency for the SMA spring isolator with a near-zero stiffness.

7. Conclusion

In this paper, one-dimensional shape memory effect modeling of SMA is carried out based on Ginzburg–Landau's theory. A constitutive model for shape memory alloy spring as obtained by combining the theory of mechanical spring is used in expressing the vibration isolation system. At last, simulation is performed to prove the isolation system based on the SMA spring and is capable of narrowing down the resonant frequency. A theoretical method for estimating the equivalent stiffness of the SMA spring is given. Several numerical results are shown in the second part of the simulation, and the influence of frequency and amplitude on equivalent stiffness is also studied.

Future Considerations:

Investigating the influence of forcing frequency alongside amplitude and applied force could provide deeper insights into resonance and mode coupling phenomena.

Detailed phase-space analysis and bifurcation studies could help delineate stable and unstable response regimes, particularly at high energy levels.

Incorporating damping and nonlinear restoring forces into the model would enhance the realism and applicability of the simulation to practical systems.

Abbreviations

SMA	Shape Memory Alloy
QZS	Quasi-Zero Stiffness

Author Contributions

Rabiu Ahmad Abubakar is the sole author. The author read and approved the final manuscript.

Conflicts of Interest

The author declears no conflicts of interest.

References

[1] Yuryev GS. Vibration Isolation of Precision Instruments. *Russ Acad Sci Sib Branch, Inst Nucl Phys Press Novosib*. Published online 1991: 89-146.

[2] Harris CM, Piersol AG. *Harris' Shock and Vibration Handbook*. Vol. 5. New York: McGraw-Hill.; 2002.

[3] Rivin EI, Rivin EI. Passive vibration isolation. *New York: Asme press*. 2003: 235-538.

[4] Le TD, Ahn KK. A vibration isolation system in low frequency excitation region using negative stiffness structure for vehicle seat. *J Sound Vib*. 2011; 330(26): 6311-6335.

[5] Zhou N, Liu K. A tunable high-static–low-dynamic stiffness vibration isolator. *J Sound Vib*. 2010; 329(9): 1254-1273.

[6] Garoi, F. W, J., Ju L, Jacob J, Blair DG. Passive vibration isolation using a Roberts linkage. *Rev Sci Instrum*. 2003; 74(7): 3487-3491.

[7] Beggs J. S. *Advanced Mechanism*. Macmillan. NewYork: Macmillan 1966.

[8] Alabuzhev PM, Rivin EI. Vibration protection and measuring systems with quasi-zero stiffness. *CRC Press*. Published online 1989.

[9] Carrella, A. et al. On the force transmissibility of a vibration isolator with quasi-zero-stiffness. *J Sound Vib*. 2009; 322(4-5): 707-717.

[10] Krishna Y, U. S. Semi-active vibration isolation using a near-zero-spring-rate device: steady state analysis of a single-degree-of-freedom model. *Proc Inst Mech Eng Part D J Automob Eng*. 2009; 11(223): 1395-1403.

[11] Xiuting S, Jian X, Xingjian J, Li C. Beneficial Performance of a Quasi-Zero- Stiffness Vibration Isolator with Time-Delayed Active Control. *J Sound Vib*. 82: 32-40.

[12] Zhou J, Xu D, Bishop S. A torsion quasi-zero stiffness vibration isolator. *J Sound Vib*. 2015; 338: 121-133.

[13] Zhou J et al. Nonlinear dynamic characteristics of a quasi-zero stiffness vibration isolator with cam–roller–spring mechanisms. *J Sound Vib*. 2015;.346: 53-69.

[14] Zheng, Y. et al. Design and experiment of a high-static–low-dynamic stiffness isolator using a negative stiffness magnetic spring. *J Sound Vib*. 2016; 360: 31-52.

[15] Sun X, X. J. Multi-direction vibration isolation with quasi-zero stiffness by employing geometrical nonlinearity. *Mech Syst Signal Process*. 2015; 62–63(October): 149-163.

[16] Yang J, Y P. Dynamics and power flow behavior of a nonlinear vibration isolation system with a negative stiffness mechanism. *J Sound Vib*. 2013; 332(1): 167-183.

[17] Yiu YC. Shape-memory alloy isolators for vibration suppression in space applications. *Sp Syst Div*. Published online 1995: 0173-15.

[18] Saadat S, Noori M, Davoodi H, Hou Z, Suzuki Y, Masuda A. Using NiTi SMA tendons for vibration control of coastal structures. *Smart Mater Struct*. 2001; 10(4): 695.

[19] Williams K, Chiu G, Bernhard R. Adaptive-passive absorbers using shape-memory alloys. *J Sound Vib*. 2002; 249(5): 835-848.

[20] Lagoudas DC, Khan MM, Mayes JJ, Henderson BK. Pseudoelastic SMA spring elements for passive vibration isolation: Part II–Simulations and experimental correlations. *J Intell Mater Syst Struct*. 2004; 15(6): 443-470.

[21] Araki Y et al. Integrated mechanical and material design of quasi-zero-stiffness vibration isolator with superelastic Cu–Al–Mn shape memory alloy bars. *J Sound Vib*. 2015; 358: 74-83.

[22] Wang L, Zhou C, Feng C. Nonlinear differential equation approach for the two-way shape memory effects of one-dimensional shape memory alloy structures. In: *International Conference on Smart Materials and Nanotechnology in Engineering (Pp. 74931Z-74931Z). International Society for Optics and Photonics.*; 2009: 74931Z-74931Z.

[23] Falk F, Konopka P. Three-dimensional Landau theory describing the martensitic phase transformation. *shape-memory Alloy J Phys Condens Matter*. 1990; 2(1): 61.

[24] Bales GS, Gooding RJ. Interfacial dynamics at a first-order phase transition involving strain: dynamical twin formation. *Phys Rev Lett*. 1991; 67(24): 3412.

[25] Sun S, Rajapakse RKND. Simulation of pseudoelastic behaviour of SMA under cyclic loading. Computational Materials Science. *J Phys Condens Matter*. 2003; 28(3): 663-674.

[26] Wang L, Melnik R V. Nonlinear dynamics of shape memory alloy oscillators in tuning structural vibration frequencies. *Mechatronics*. 2012; 22(8): 1085-1096.

[27] Abubakar RA, Yutian H, Wang F, Wang L. Modeling and Experimental Validation of the Hysteretic Dynamics of Shape Memory Alloy Springs. *Int J SMART Sens Intell Syst*. 2020; 30(1): 1-9.